PROCEEDINGS, 42nd Workshop on Geothermal Reservoir Engineering
Stanford University, Stanford, California, February 13-15, 2017
SGP-TR-212

Modeling Microseismic Activity in the Newberry Enhanced Geothermal System

Christopher S. Sherman and Joseph P. Morris

Lawrence Livermore National Laboratory, 7000 East Ave, Livermore, CA 94550

sherman27@llnl.gov

Keywords: Microseismicity, Geomechanics, Modeling

ABSTRACT

During the stimulation of an enhanced geothermal system (EGS), the timing and location of induced microseismicity is one of the key indicators for the stimulation's effectiveness. In our analysis, we constructed a 3D, fully-coupled, thermo-hydraulic-mechanical (THM) model of the Newberry EGS, which includes a realization of a discrete fracture network (DFN), using the GEOS platform (Settgast et al., 2016; Sherman et al., 2016). We perform a statistical analysis of the shear and normal dislocations on the DFN to estimate the degree of microseismic activity within voxelized regions of the model. This method properly quantifies the effects of microseismic activities that would otherwise require element sizes too small to be computationally tractable. We then apply the same algorithm to an equivalent estimate of activity using the field microseismic catalog. Using the predicted pressure, flow rate, and microseismic activity data, we calibrate our model against a set of hydroshearing stimulations in the region performed by AltaRock during 2012 and 2014.

1. INTRODUCTION

In this paper, we discuss our efforts to develop a numerical model of microseismic activity at the Newberry EGS test site, which is located in central Oregon and is operated by AltaRock Energy, Inc. under a department of Energy grant (Cladouhos et al., 2009; Cladouhos et al., 2015; Cladouhos et al., 2016). During 2012 and 2014, AltaRock attempted to stimulate the reservoir using hydroshearing, a process in which fluid is injected at pressures below the threshold for hydraulic fracturing, but high enough to trigger shearing and dilation on pre-existing fracture surfaces. The range of design parameters tested throughout these stimulation attempts, combined with the large amount of microseismic and pumping data, make this an excellent target for the model calibration.

A previous study by Rinaldi et al. (2015) attempted to model the hydroshearing process at Newberry using the using the TOUGH2 reservoir simulator code coupled to the Finite Difference geomechanics code FLAC3D. Their approach relied on a modeling the mechanics and flow in the reservoir as a continuum problem, with an empirical model to account for permeability changes due to hydroshearing. In contrast, our approach, which was first proposed by Sherman et al. (2016), is to explicitly model the hydroshearing process in the fractured reservoir, to model the associated changes in fluid permeability using first-principles, and to simultaneously recover the geophysical signals required to verify the efficacy of our model.

2. NUMERICAL METHODOLOGY AND DATA PROCESSING

The numerical work presented in this paper was completed using the massively parallel, multiphysics code GEOS, which is developed by Lawrence Livermore National Laboratory. We use a fully-coupled thermal-hydro-mechanical (THM) model to simulate the hydroshearing process in a discrete fracture network (DFN) and to predict its associated microseismic response.

2.1 Thermal-hydro-mechanical model

The THM modeling capabilities in GEOS have been used to simulate processes ranging from hydraulic fracture propagation in an unconventional oil reservoir (Settgast et al., 2014) to thermal effects on fluid flow in a fractured geothermal reservoir (Guo et al., 2016). The model uses a Finite Element (FE) approach to solve for the thermo-mechanical effects in the rock, and uses a Finite Volume approach to solve for fluid and heat flow in the rock matrix and fracture network. Depending on the time scale of the application and the expected degree of physical coupling, we use a combination of explicit and implicit time-stepping schemes to advance the problem. Contact mechanics in the fracture network is handled using a penalty approach, with frictional properties governed by either a Coulomb or rate and state formulation and hydraulic conductivity governed by a Barton-Bandis model. Fracture propagation in the model is allowed along pre-existing faces in the FE mesh, and is governed by linear elastic fracture mechanics (LEFM).

2.2 Microseismic model

Modeling the development of microseismicity over an entire geothermal reservoir faces challenges ranging from the limited geomechanical data available for the model design to the need for balance between numerical cost and fidelity. Based on earthquake scaling relationships we expect that microseismic events with magnitudes in the range $-3 < M_w < 0$ should occur on slip patches that are on the order of 0.1 to 10 m in length (Cowie and Scholz, 1992). Modeling the microseismic activity as discrete, fully-coupled events requires a model with a numerical resolution that is a fraction of the minimum desired slip patch size, and would require an equivalently high resolution geostatistical model to be accurate. Using this sort of approach over the entire reservoir, which is on the order of 1 km in size, would require on the order of a billion elements and would be prohibitively expensive to run. On the other hand, while it requires significantly less computational resources to run, modeling the microseismicity as embedded point sources introduces

challenges regarding the degree of coupling to the larger geomechanical model (Sherman et al., 2016). These coupling terms, which under the point-source approximation are assumed to be weak, control the feedback mechanism that is necessary for constraining the total energy release and magnitude-scaling relationships in the model.

In our analysis, we use an intermediate approach proposed by Sherman et al. (2016) to approximate the microseismic response within a discrete fracture network (DFN), with element sizes up to a few times larger than the target slip patch size. To achieve this, the model is brought into an exceptionally quiet state using an implicit initialization scheme that then allows us to track the development of slip discontinuities within the network with sub-micron precision during the hydraulic stimulation. The moment tensor contributions for each element along a surface are calculated using the closed-form solutions for a double-couple and crack-opening mechanisms given by Aki and Richards (2002).

As a consequence of using a relatively large element size to reduce the computational cost, the energy released through individual seismic events and through aseismic slip are combined into a single, smooth estimate of moment release. Therefore, to use this model, it is necessary to estimate the average seismic conversion factor, α:

$$\alpha = M_{o,seismic}/M_{o,total}\ , \tag{1}$$

where $M_{o,seismic}$ is the cumulative seismic moment released from field observations and $M_{o,total}$ is the estimate of total moment release from the model. After scaling the total moment release for the system, it is possible to invert the distribution of seismic slip in the system for the Gutenberg–Richter *a* and *b* values by assuming an empirical scaling relationship between slip magnitude and patch size [e.g.: Cowie and Scholz (1992)].

2.3 Microseismic response estimates

One the main challenges facing a direct, quantitative comparison between the numerical microseismic model and field observations is that the seismic conversion factor is in fact a distribution of values that is dependent on the small-scale, unresolved heterogeneity present in the system. Based on the relative scales between the numerical model and field measurements, we select a reference volume, *V*, over which we expect the conversion factor to be uniform, and construct the voxelized cumulative moment release function, $\widetilde{M}$:

$$\widetilde{M}(\boldsymbol{X},t) = \Phi * \frac{1}{V}\iiint M_o(\boldsymbol{X}+\boldsymbol{\xi},t)d\boldsymbol{\xi}, \tag{2}$$

where $\boldsymbol{X}$ and $\boldsymbol{\xi}$ are position, *t* is time, Φ is a smoothing kernel, * is the convolution operator, and M_o is either the moment release estimate from the numerical model or the field microseismic observations. We calculate the corresponding moment release rate functions, $\dot{M}$, using a forward finite-difference operator:

$$\dot{M}(\boldsymbol{X},t) = \frac{\widetilde{M}(\boldsymbol{X},t+\Delta t)-\widetilde{M}(\boldsymbol{X},t)}{\Delta t}, \tag{3}$$

where Δ*t* is the characteristic time step. While the values of $\widetilde{M}$ and $\dot{M}$ may be directly compared in space and time, we found that it is often more convenient to project the results into a two-dimensional image. For instance, we may look at the projection of the moment release rate estimates in the *x*-*t* plane, $\dot{M}_x$:

$$\dot{M}_x(x,t) = \iint \dot{M}(\boldsymbol{X},t)dydz, \tag{4}$$

where *y* and *z* are the out of plane dimensions.

An example of this processing technique, applied to a simple numerical model of a vertical hydraulic fracture propagating through a DFN, is given in Figure 1. By tracking the moment release rates in each direction, we can predict the timing, location, and intensity of microseismic events. In addition, we are able to determine the correlation between the microseismicity and the growth of the hydraulic fracture in the system.

3. NEWBERRY MODEL DEVELOPMENT

To develop a calibrated model of the Newberry EGS site, we considered three distinct classes of models: first, a very large-scale mechanical model for estimating the local stress state; second, a set of small-scale models for testing the hydraulic properties of the DFN; and third, a set of large-scale for testing fluid injection properties, boundary condition effects, etc. As a target for these simulations, we also calculated the microseismic response estimates discussed in the previous section.

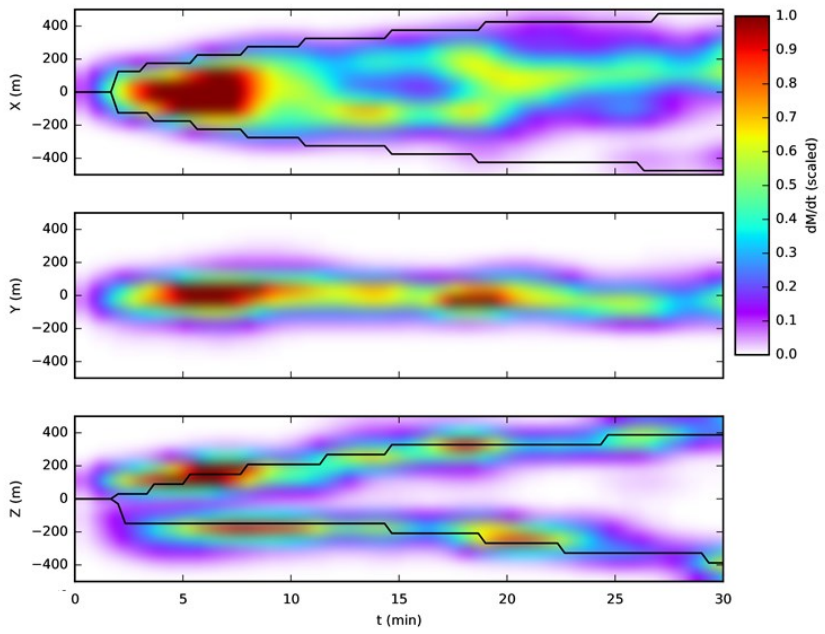

Figure 1: The estimated microseismic moment release rates in response to a hydraulic fracture propagating through a DFN. The solid black lines superimposed on the images indicate the measured extents of the fracture with time.

3.1 Large-scale stress model

The flow of fluid and the development of new fracture surfaces in a DFN is very sensitive to variations in the in-situ stress state. To develop a consistent estimate of stress in the Newberry reservoir, we constructed a large-scale mechanical model using boundary and initial conditions estimated from borehole measurements by Davatzes et al. (2011) and Cladouhos et al. (2015). The model is 10 x 10 x 10 km in size, includes the measured surface topography, and has mechanical properties estimated from the seismic tomographic study by Matzel et al. (2014). An image of the model, which shows the distribution of the shear modulus in the system, is given in Figure 2. We used an implicit mechanics solver to estimate the stress state throughout the reservoir, which we use as an initial condition for the smaller-scale models that include fluid flow

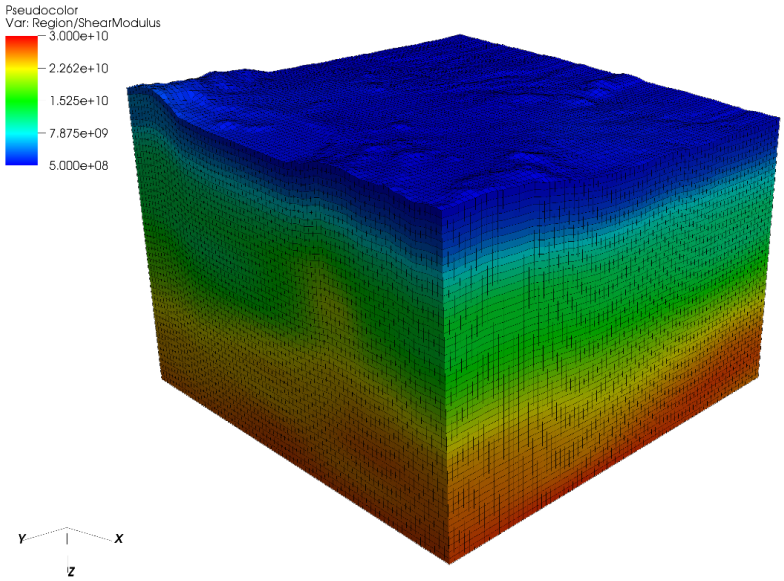

Figure 2: An image showing the distribution of the shear modulus in the large-scale (10 x 10 x 5 km) Newberry stress model.

3.2 Small-scale DFN models

The behavior of the contact model in the DFN controls the rate that fluid and other materials may flow into the reservoir, the potential development of hydraulic fractures, and the degree and extent of microseismic activity. To test for this behavior, we construct a small (1 x 1 x 1 km) model of the Newberry reservoir at a depth of 3 km, centered on the location of the NWG 55-29 well. As before, the material properties were estimated from the seismic tomography data, and the initial stress state was estimated from the large-scale model. To limit their computational cost, these models used a coarse grid size of 50 m in the core region and ignore thermal effects.

The discrete fracture networks used in these models were designed using borehole measurements from Davatzes et al. (2011), which suggest that there are two major joint sets in the region, each striking north-south, with the first dipping 50º to the east and the second dipping 50º to the west. Each realization of the DFN is constructed by randomly placing joints from the dominant sets throughout the model, snapping them to the underlying mesh, and filtering them to avoid bad geometric arrangements. We used a penalty stiffness for these faces of 10 GPa, a static coefficient of friction of 0.6, and rate and state parameters with *(a-b)* equal to either -0.005 (rate-weakening) or 0 (Coloumb friction). Because we are only able to include a subset of the largest potential fractures present in the system, we use a pressure-dependent leakoff model to account for the fluid loss into feature not explicitly represented in the system.

We injected fluid into a set of pre-fractured elements in the center of the models, using either a constant flow rate boundary condition or a time-varying pressure boundary condition. To test the models for their susceptibility to hydraulic fracturing, we oriented the injection site to be normal to the principle stress. An example of one of these models, where we injected fluid at a constant pressure of 32 MPa into a highly conductive reservoir over 30 minutes, is given in Figure 3.

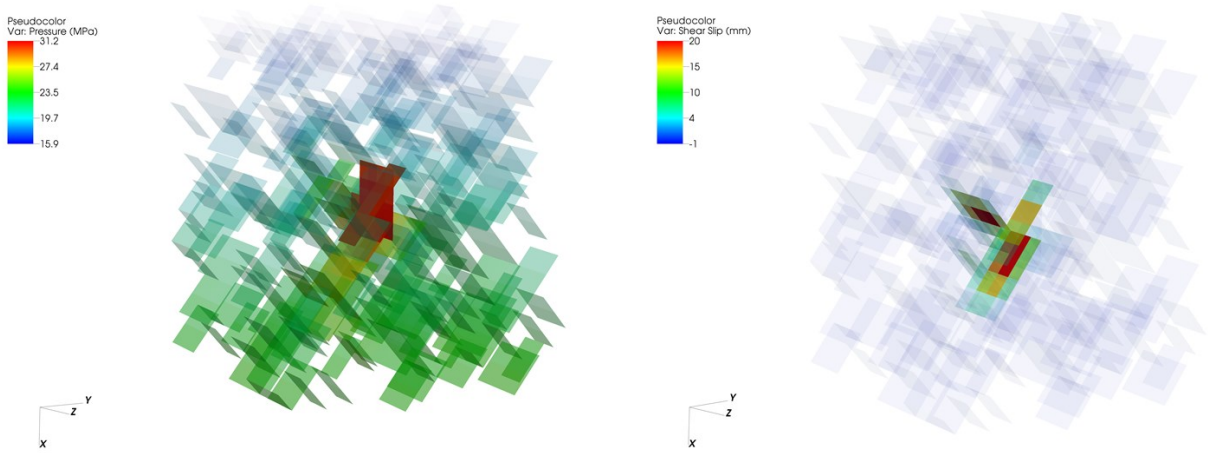

Figure 3: Measured fluid pressure (left) and shear slip (right) within the DFN for a small-scale test model after 30 minutes of pumping.

In these models, we track the rate at which the fluid pressure front moves through the system to calibrate the Barton-Bandis joint parameters and the leakoff model. We also track the normal opening and shear slip within the DFN, which are related to crack opening and double-couple microseismic failure modes, to calibrate the frictional contact model. As expected, we found that the movement of the pressure front and the extent of slip within the DFN are well correlated. In addition, we found that while using a rate-weakening friction contact model may alter the timing of microseismic activity in the model, it did not have a strong effect on the total moment release in the model.

3.3 Large-scale DFN models

To advance the calibration of the Newberry hydroshearing model in GEOS, we are currently testing a set of large-scale simulations with more realistic fluid injection schemes. The core region in these models is 2 x 2 x 2 km in size, at a depth of 2.5km and centered around the location of the same 2012 hydroshearing test in well NWG 55-29, and have a much higher resolution of 12.5 m. A lower-resolution region expands upwards toward the surface, matching the measured topography of the site, and extends outwards 1 km in the remaining directions. The material properties, initial stress state, and DFN characteristics are the same as those in the small-scale models. Because these models are much more expensive to run, our initial tests assumed an axis of symmetry in the East-West direction and ignored thermal effects to reduce cost.

The design of the fluid injection scheme in the large-scale models is complicated by the combination of large sections of perforated casing throughout the well, a possible casing failure, and a set of perforation shots conducted in the later stages of the stimulation efforts (Cladouhos et al., 2015). To simplify this behavior, we consider two end-member models where fluid is injected into either through the slotted casing *or* through a perforation cluster. By comparing the calculated injection pressures and flow rates into the model against field measurements, and their associated microseismic signatures, we expect to determine the appropriate balance between these modes.

Figure 4 gives an overview of a large-scale model where we inject fluid at a constant rate of 0.005 m^3/s into a perforation cluster at a depth of 2.5 km. After 17 hours of pumping, the fluid pressure has reached an equivalent wellhead pressure of about 8 MPa, and the pressure front has only moved out a small distance into the formation. The measured microseismic response over this time frame is similarly limited, so we do not include it here. As we refine the behavior of these large-scale models, we plan to increase the simulation time to the scale of weeks, and to better match the as-pumped injection rates.

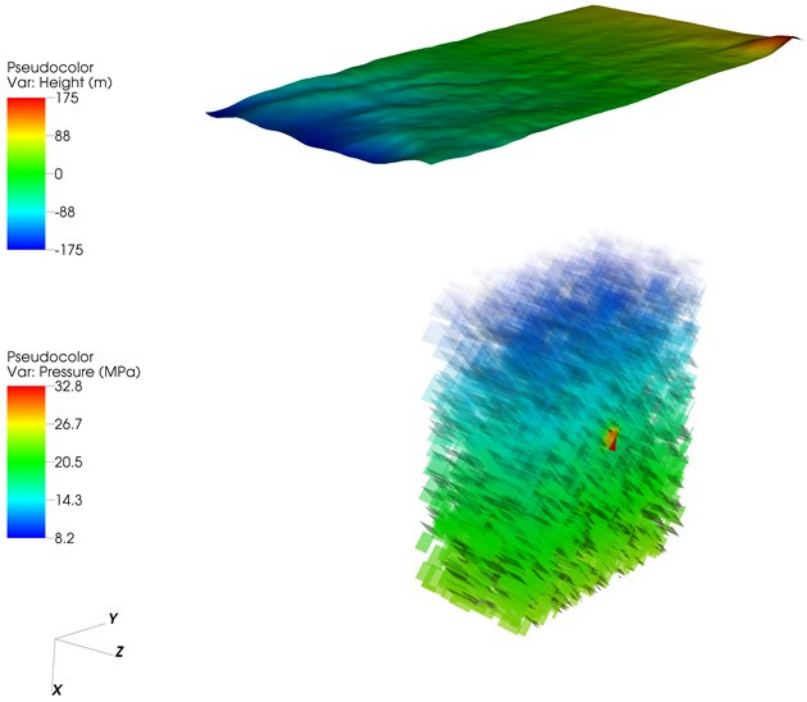

Figure 4: The measured pressure in a large-scale Newberry test model after 17 hours of pumping, and the surface topography over the site.

3.4 Field microseismic response targets

To provide targets for the numerical microseismic model calibration, we processed sections of the Newberry microseismic catalog, published by Lawrence Berkeley National Laboratory. Figure 5 shows an example of the calculated microseismic moment release rate measured at the site during the Phase 2, Round 1 stimulation from September 28th to October 18th 2014 (before the perforation shots). To prevent the largest events in the catalog from dominating the calculated microseismic response, we instead use the moment magnitude as the input to Equation 2. This figure shows that the microseismic energy is release rate is nearly symmetric in the horizontal direction, and is more diffuse in the vertical direction.

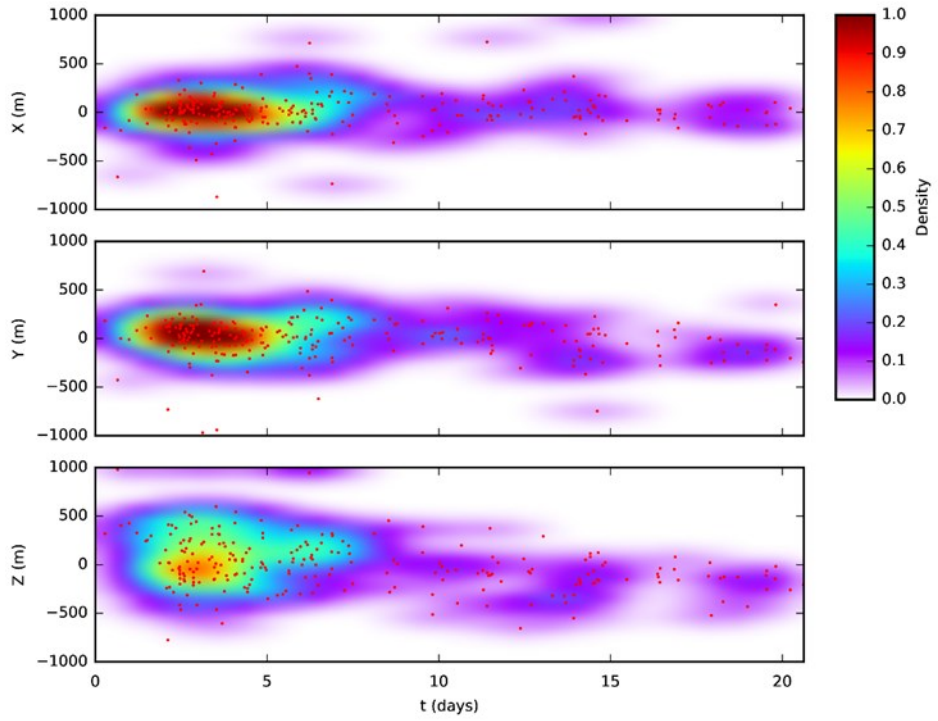

Figure 5: Microseismic moment release rate targets for the Phase 2, Round 1 stimulation at Newberry. The red points show the location of individual event in the LBNL catalog.

5. CONCLUSIONS

In this paper, we have developed an approach for modeling the hydroshearing stimulations at the Newberry EGS site using a fully coupled THM model, with an explicitly represented DFN. We have also developed a method for recovering the microseismic activity directly from the model and an approach for seismic processing that is consistent with field measurements. Moving forward, we are continuing the calibration process of the large-scale models against the available pumping and microseismic data, incorporating thermal measurements into the models, and are working to improve the efficiency of the simulations.

ACKNOWLEDGMENTS

This work was performed under the auspices of the U.S. Department of Energy by Lawrence Livermore National Laboratory under contract DE-AC52-07NA27344. The Newberry microseismic catalog used in this paper was based upon work supported by the U.S. Department of Energy, Office of Energy Efficiency and Renewable Energy (EERE), Office of Renewable Power, Geothermal Technologies Office, by Lawrence Berkeley National Laboratory under Award Number DE-AC02-05CH11231.

REFERENCES

Aki, K., and Richards, P.G.: Quantitative Seismology, 2nd Ed, Sausalito: University Science Books, (2002).

Cladouhos, T.T., Petty, S., Nordin, Y., Garrison, G., Uddenberg, M., Swyer, M., Grasso, K., Stern, P., Sonnenthal, E., Rose, P., Foulger, G., and Julian, B.: Results from Newberry Volcano EGS Demonstration 2010 – 2014, Geothermics, **63**, (2016), 44-61.

Cladouhos, T., Petty, S., Larson, B., Iovenitti, J., Livesay, B., and Baria., R.: Toward More Efficient Heat Mining: A Planned Enhanced Geothermal System Demonstration Project, GRC Transactions, **33**, (2009), 165-170.

Cladouhos, T.T., Petty, S., Swyer, M.W., Uddenberg, M.E., Grasso, K., and Nordin, Y.: Newberry EGS Demonstration Project, Phase 2.2 Report, AltaRock Energy (2015).

Cowie, P.A., and Scholz, C.H.: Displacement-length Scaling Relationship for Faults: Data Synthesis and Discussion, J. of Structural Geology, **14**, (1992), 1149-1156.

Davatzes, N.C., and Hickman, S.H.: Preliminary Analysis of Stress in the Newberry EGS Well NWG 55-29, GRC Transactions, **35**, (2011), 323-332.

Guo, B., Fu, P., Hao, Y., Peters, C.A., and Carrigan, C.R.: Thermal Drawdown-induced Flow Channeling in a Single Fracture in EGS, Geothermics, **61**, (2016), 46-62.

Matzel, E., Templeton, D., Petersson, A., and Goebel, M.: Imaging the Newberry EGS Site using Seismic Interferometry, *Proceedings*, Thirty-Ninth Workshop on Geothermal Reservoir Engineering Stanford University, Stanford, CA (2014).

Rinaldi, A.P., Rutqvist, J., Sonnenthal, E.L., and Cladouhos, T.T.: Coupled THM Modeling of Hydroshearing Stimulation in Tight Fractured Volcanic Rock, Transport in Porous Media, **108**, (2015), 131-150.

Settgast, R.R., Johnson, S., Fu, P., Walsh, S., and White., J.: Simulation of Hydraulic Fracture Networks in Three Dimensions Utilizing Massively Parallel Computing Resources, *Proceedings*, Unconventional Resources Technology Conference, Denver, CO (2014).

Sherman, C.S., Templeton, D.C., Morris, J.P., and Matzel, E.: Modeling Induced Microseismicity in an Enhanced Geothermal Reservoir, *Proceedings*, 50th US Rock Mechanics Symposium, Houston, TX (2016).